# PROPERTIES OF BULK MATERIALS FOR HIGH-TEMPERATURE AIR-SAND HEAT EXCHANGERS

**Torsten Baumann[2], Cristiano Boura[1], Julian Eckstein[1], Jan Dabrowski[1], Joachim Göttsche[1], Bernhard Hoffschmidt[1], Stefan Schmitz[1] and Stefan Zunft[2]**

[1] Solar-Institut Jülich / FH Aachen, Heinrich-Mußmann-Str. 5, D-52428 Jülich, Germany

[2] German Aerospace Center (DLR), Pfaffenwaldring 38-40, D-70569 Stuttgart, Germany

## 1. Introduction

Dispatchability of CSP and a further reduction of levelized electricity costs are strong incentives for the development of cost-efficient technical solutions for thermal storage systems. A heat storage system using fine-grained particles as its storage material is a technology option that offers novel low-cost solutions. The implementation of this concept however depends on a viable concept for an air-to-particle heat exchanger, a component that is needed to heat up the particle flow and that is not available on the market today. Solar-Institut Jülich (SIJ) and the German Aerospace Centre (DLR) are developing and testing a new air-to-particle heat exchanger (Warerkar et al., 2009). Relevant problems include high temperature gradients in sand and frame structure, the pressure drop through the heat exchanger, the thermodynamic behavior and the fluid dynamic interaction within the bulk material.

In this paper open questions on material properties of the sand-like inventory are addressed. High requirements are placed on the particulate materials used in sand-air heat-exchanger to ensure a smooth and efficient operation for many years. Hence, a detailed analysis of candidate bulk materials and their properties are of ample importance for the development of the technology. The focus of this work is put on properties like effective thermal bulk conductivity, thermal shock resistance, and attrition aspects.

## 2. Sand Storage Concept

The sand storage concept in an open-volumetric receiver solar tower (Hoffschmidt, 1997 and 2003) involves an air-sand heat exchanger unit as the most cost-relevant component, a component that is not available on the market today. First experience with a small 15 kW prototype has been reported (Warerkar et al., 2009). The air-sand heat exchanger concept (Fig. 1) assumes a cross flow of air and sand, where the sand is moving vertically, driven by gravity only, and the air is passing horizontally through the sand driven by a fan. The heat exchanger volume must be enclosed by filter walls at the air inlet and exit areas in such a way that the bulk material always fills the volume completely and that it does not penetrate the filter walls.

First results have been obtained in a previous project where a 15 kW sand-air heat exchanger was built and operated. Theoretical studies have shown that good thermal performance is achievable at moderate pressure drop (Warerkar et al., 2009). The ongoing project Hitexstor advances the technology by looking at properties of material candidates and further detail design options for the heat exchanger.

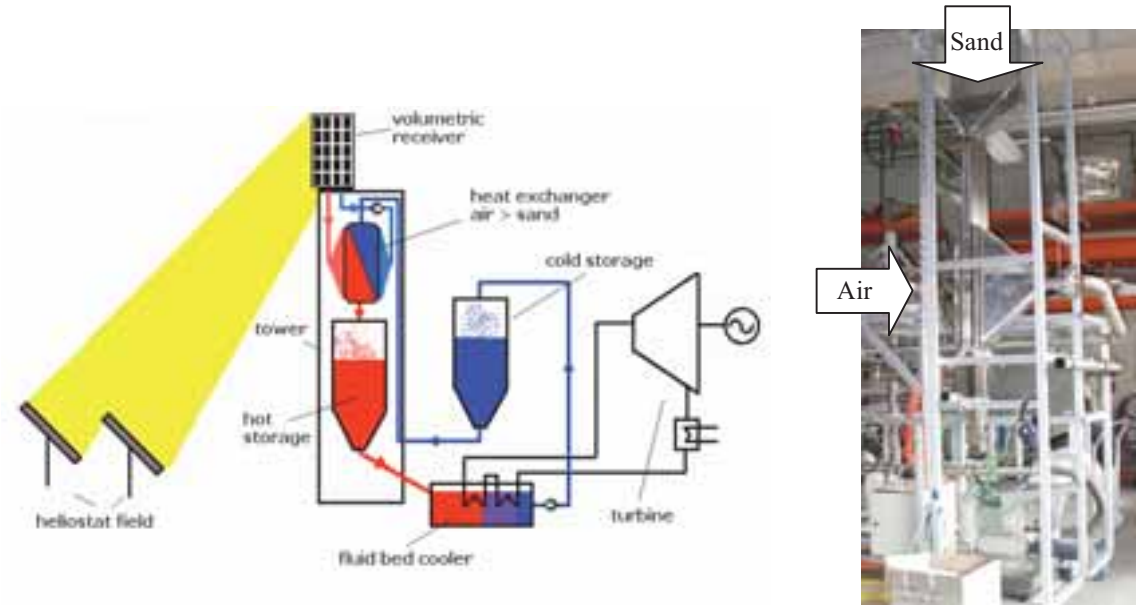


**Fig. 1: Sand storage concept for solar power towers [1] (left) and 15 kW heat exchanger prototype (right) [2]**

## 3. Properties of short-listed bulk materials

*Thermal Conductivity*

The thermal conductivity of the bulk is one of the determining factors for the thermal performance of the heat exchanger. The knowledge of this material parameter is therefore crucial for its design.

Measurements of effective thermal bulk conductivity have been performed with the method of heated wire in a Netzsch TCT 426 thermal conductivity analyzer (see figure 2 below). Bulk conductivity was measured in a temperature range from room temperature to 800°C. The materials used in the tests include the most promising material candidates as listed in table 1 below.

**Table 1: Grain sizes of tested granular materials**

| Material | Volumetric mean grain size [mm] | Standard deviation [mm] |
|---|---|---|
| Sintered bauxite | 1.49 | ± 0.26 |
| | 0.56 | ± 0.09 |
| Alumina grinding balls | 2.01 | ± 0.50 |
| | 1.17 | ± 0.20 |
| Basalt | 2.89 | ± 1.08 |
| Quartz flint | 2.02 | ± 0.57 |
| Quartz sand | 0.80 | ± 0.18 |
| Normal corundum F14 | 1.83 | ± 0.42 |
| NC F16 | 1.61 | ± 0.36 |

In figure 3 below, the measured results are shown. Though the thermal conductivity of the solid materials span a wide range from 2 W/mK (e.g. basalt at 800°C) to 20 W/mK (e.g. alumina at 20°C), the corresponding effective bulk conductivities turn out to be in a narrow range between 0.2 to 0.3 W/mK for low temperatures and 0.5 to 0.8 for high temperatures. Hence, the solid's thermal conductivity is of minor importance for the bulks thermal behavior.

The increase of effective conductivity with temperature is attributed to the increasing contribution of thermal radiation on the apparent conductivity at higher temperatures. As can be seen in figure 3, a larger grain size

of the same material leads to a higher effective conductivity. Here, the underlying effect is seen in the reduced number of particle contacts reducing the conductive heat resistance with larger particles. Also, the radiative heat resistance is reduced with a smaller number of particles on a given distance.

**Fig. 2: Sintered bauxite in the TCT 426 hot wire device**

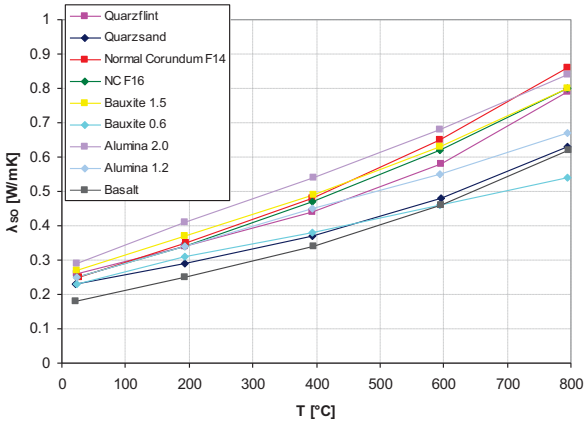


**Fig. 3: Effective heat conductivity of various granular materials**

*Thermo-shock resistance*

To ensure stable and predictable operating conditions of the system over the materials lifetime, degradation and the resulting reduction of grain size must be avoided, as this would negatively affect pressure drop and the flow behavior of the bulk. One of the potential origins of such failures is thermal shock occurring in the heat exchanger during charge operation and must therefore be considered. To this end, a thermal cycling of a number of materials has been performed.

Cyclic thermo-shock tests have been applied to the materials through heating to approx. 810°C, water quenching at 20°C and subsequent drying at 110°C. With the help of the image analysis system Powder Shape, grain size distribution was determined after five, ten and thirty cycles and then compared with untreated specimens.

As a result it turns out that for the ceramic materials, like sintered bauxite or alumina, the grain size distribution remains almost unaffected from this treatment. This is illustrated in figure 4 below for alumina, where the almost unchanged curves indicate a good suitability and a high lifetime expectancy with cyclic thermal loads.

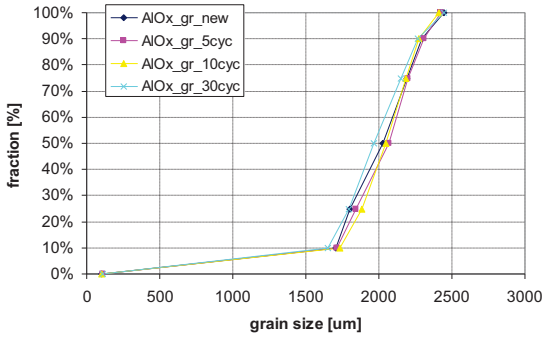


**Fig. 4: Cumulated grain size for alumina after 0, 5, 10 and 30 cycles**

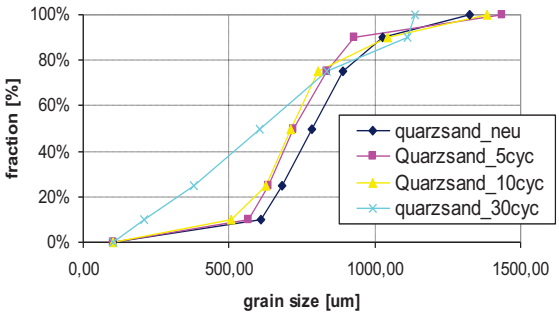


**Fig. 5: Cumulated grain size for quartz sand after 0, 5, 10 and 30 cycles**

In contrast, the investigated natural products have a higher sensitivity to thermal cyling. As can be seen from Fig. 5, quartz shows a pronounced granular disintegration, becoming visible from an increased fraction of fine particles after 30 cycles. Here, thermally induced stress exceeds the mechanical strength of the material and thus leads to breakage of the grains. This is further amplified by the quartz inversion, occurring at

approx. 573°C.

Less pronounced, but still visible effects of degradation have been determined for basalt and normal corundum. A possible damage mechanism could again result from the typically existing quartz-phase in the grain. Hence, the use of natural products containing quartz phases in general, and specifically quartz products, bears the risks of limited lifetime when operated with high temperature gradients and with temperatures around the quartz inversion point.

### *Attrition behavior*

The relative movement of the particles is another origin for potential changes in grain size distribution, with possible effects on flow behavior of the bulk and air-side pressure drop. To limit such risks, attrition tests were performed in a ring shear cell as shown in figure 6 below. The device consists of a ring channel filled with the granules and a matching cover plate. The bulk material is densified by the plate with a specified normal force, inducing an attrition load in the bulk. By rotation of the cover plate, an additional shear stress is generated. A perforated plate is installed at the bottom of the ring channel, keeping the lower layer of particles in place to achieve the formation of a shear zone in the bulk of 20-30 mm width.

The failure zone, in which attrition occurs due to a high strain rate, is assumed to have a width of 6 to 10 mm (Bridgwater, 2007, Ghadiri et al., 2000). An the initial mean grain size of the specimens ranging from 1.5 to 2.9 mm implies that almost all particles are located in the failure zone. All tests have been conducted with a normal force of 2 kN, inducing a normal force of 84 kPa in the bulk, and with a rotational speed of 42 rpm, corresponding to a mean velocity of 3 m/s. Attrition is quantified using a subsequent sieve analysis.

The test results are summarized in Fig. 7 below. It shows the fraction of attrition plotted versus strain rate, which is defined as ratio of shear length to sample layer thickness. Attrition is defined as mass fraction of particles smaller than their smallest initial grain size. From this diagram it can be gathered that, unlike all other tested materials, alumina grinding balls turn out to remain completely wear-free thanks to its high roundness, hardness and tensile strength. Bauxite degrades faster than quartz flints, but both materials' attritions saturate at a value around 60 % and 45 %, respectively. No such saturation effects were found for corundum and basalt within the indicated testing periods.

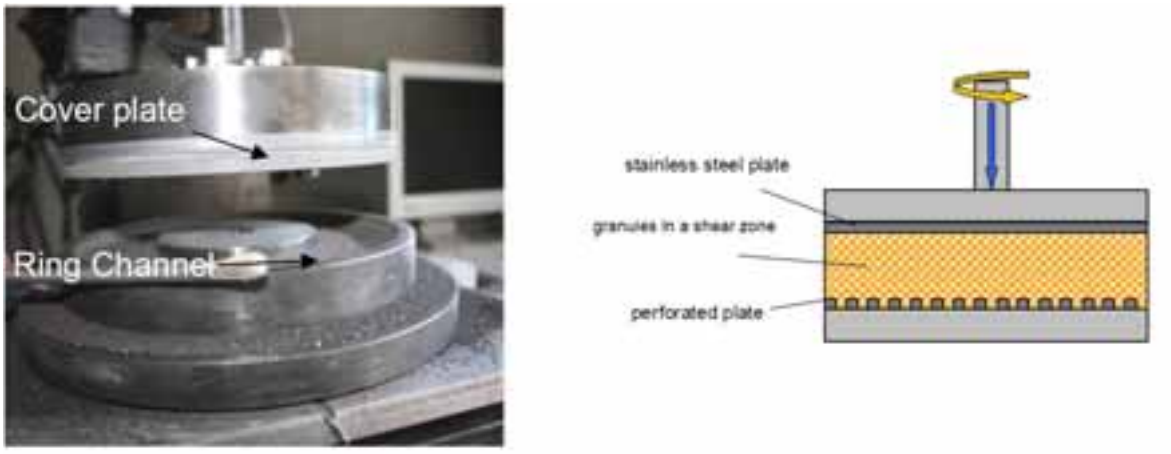


**Fig. 6: Shear cell device (left), principle of the shear cell (right)**

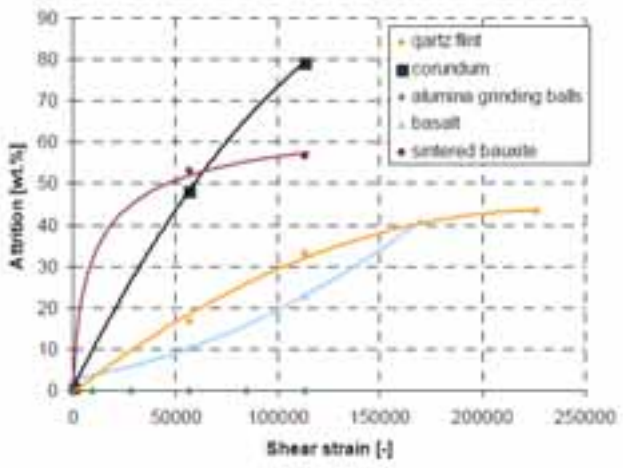


**Fig. 7: Attrition vs. shear strain for different granular materials**

The results in figure 7 can now be used to deduce statements on the long-term behavior the materials: Based on the modified Gwyn equation, an empirical correlation, the particle attrition can be related to the mechanical load condition expressed by the bulk's normal stress and shear strain in an annular shear cell (Bridgwater, 2007):

$$W = K_N \left( \frac{\sigma \Gamma^{\phi}}{\sigma_{SCS}} \right)^{\beta}, \qquad \text{(eq.1)}$$

where $W$ is the mass fraction of broken particles, $\Gamma$ the shear strain , $\sigma$ the normal stress applied to the bulk and $\sigma_{SCS}$ the tensile strength of the solids. Performing least square fits of the experimental data to this equation allows to estimate the material parameters $\beta, \Phi,$ and $K_N$. The parameters $\beta, \Phi$ describe the effect of stress and strain on attrition, respectively. $K_N$ can be interpreted as a measure of the attrition at a shear strain of unity and is called the Gwyn constant (Bridgwater, 2007). The estimated values for $\beta$, $\Phi$ and $K_N$ are listed in Table 2.

**Table 2: Material parameters for the modified Gwyn-Equation**

| Material | B [-] | Φ [-] | $K_N$ [-] |
|---|---|---|---|
| Sintered bauxite | 0.5 | 0.21 | 38.5 |
| Basalt | 2.7 | 0.5 | 135 |
| Alumina | 0.4 | 0.05 | 0.035 |
| Normal corundum | 1.45 | 0.5 | 1.79 |
| Quartz flints | 1.05 | 0.5 | 1.13 |

Further tests were conducted with the aim to quantify abrasion on a number of materials that could be used for filter walls in the air-sand heat exchanger. Candidates tested were two types of ceramic honeycombs made from Re-SiC and Si-SiC, and meshes of stainless steel. These materials were assembled onto the cover plate and sheared over the granules instead of the stainless steel plate used for attrition tests.

The test results show that abrasion on wall materials significantly depends on the combination of wall material and granular material. While honeycombs made of porous Re-SiC are almost completely destroyed by basalt and quartz flints after 3 hours under load, the dense structure of Si-SiC honeycombs exhibits high resistance to abrasion for quartz, basalt and bauxite with no evident damage after the same testing time (see Fig. 8).

The metallic meshes are partially destroyed shortly after being exposed to alumina grinding balls, as can be

seen in Fig. 9. The desintegration of the mesh structure is not due to the poor wear resistance of the stainless steel, but the mechanical interaction between the particles and the fiber ends. The mesh structure is destroyed by fibers being pulled from the mesh. The use of such meshes as filter walls is thus viable only if the mesh's fibre ends can be protected.

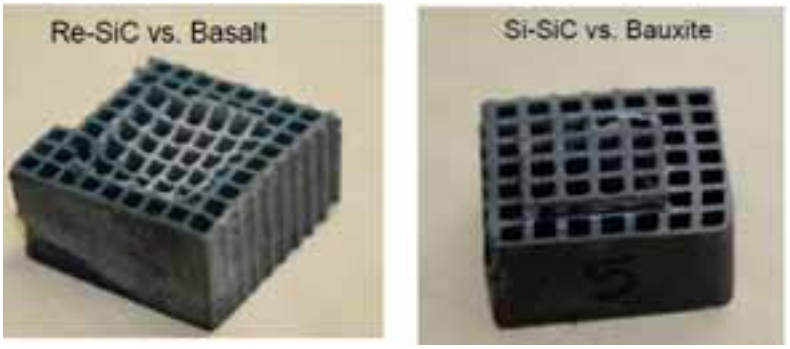


**Fig. 8: Re-SiC after abrasion by basalt (left) and Si-SiC after abrasion by bauxite (right)**

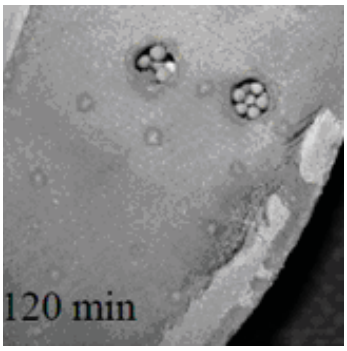


**Fig. 9: Destroyed metallic mesh after exposure to moving alumina grindig balls for 120 minutes**

### *Flow properties of particulate materials*

Fig. 10 shows the pressure drop the air flow experiences when passing through a compact bed of sand. It is the most critical performance parameter because it directly affects the parasitic energy consumption of the fan. Therefore several commercially available mineral bulk products have been examined at room temperature in a 7 cm x 7 cm x 10 cm test box, where the material was confined by wire mesh on each side. The air volume flow was measured with an orifice. Average air velocities $v_{Air}$ in front of the inlet filter were calculated. Pressure drop $\Delta_p$ of the 10 cm thick material was calculated as an average of data measured in an upward and downward flow direction after fitting the data with a second-order least-square fit.

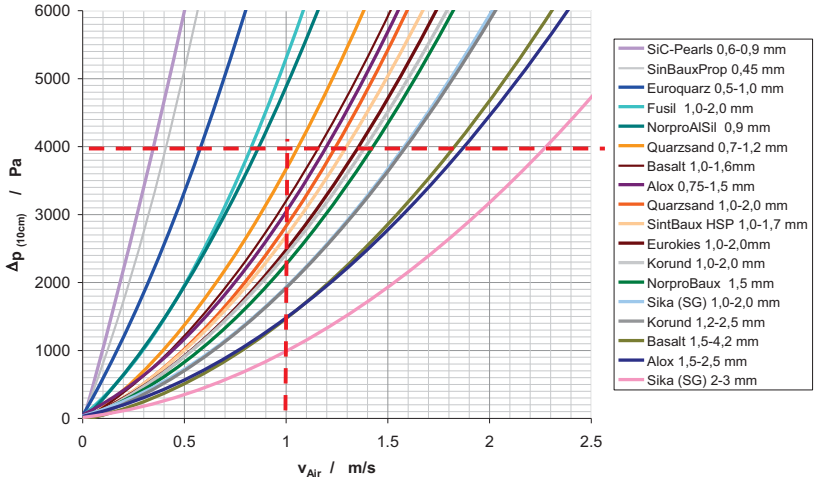


**Fig. 10: Pressure drop results**

Materials in the legend are sorted with respect to the air velocity required for a 4000 Pa pressure drop. Obviously the fine materials impose the highest pressure drop. Particle shape and the width of the particle size distribution are further relevant factors. A reasonable requirement is a pressure drop < 4000 Pa at an air velocity of 1 m/s. All materials with an average grain size > 1 mm, except for Fusil, can fulfill this condition.

In a previous experiment with a 15 kW heat exchanger unit it was observed that the sand flow was blocked when the air flow was too strong. This phenomenon is called pinning and was analyzed in more detail for six different materials:

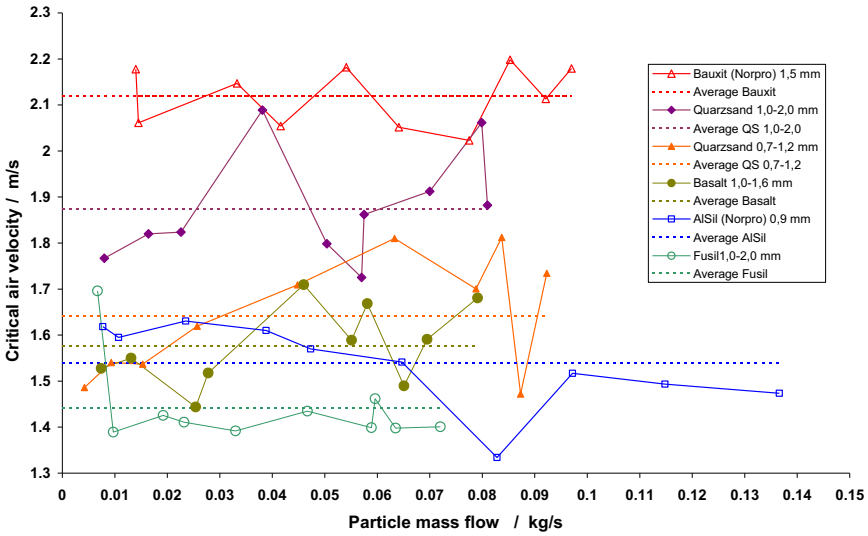


**Fig. 11: Critical air velocity for sand blocking**

In a low-temperature experimental unit the particles could be observed through a Perspex window. The critical air velocity was determined by increasing the mass flow rate up to the first observation of a void. Then the flow rate was slightly reduced until the volume filled again. Conditions were maintained for 3 minutes in order to ensure stability. The procedure was repeated with increasing particle mass flow rates. Air velocities were determined from air flow rates as in the previous experiment.

As displayed in Fig. 11, there is a considerable amount of scattering. Nevertheless, it can be observed that coarse materials are less sensitive to pinning than fine materials. Highest flow rates without blocking could be observed with the 1.5 mm round spheres of Norpro bauxite. The desired air velocity of about 1 m/s could be achieved for any examined material. There is no clear general trend that relates the critical air velocity to the sand mass flow rate. This experiment was carried out at room temperature.

Depending on air mass flow and its temperature, the moving bed is observed to undergo three phases of flow restriction, shown in Fig. 12:

- Phase 1 (Congestion): A small area at the bottom of the exit area starts to congest and stops its downward movement
- Phase2 (Blistering): At the top of the inlet area a little volume develops which is not filled with bulk material
- Phase 3 (Blockade): The bulk flow is stopped completely

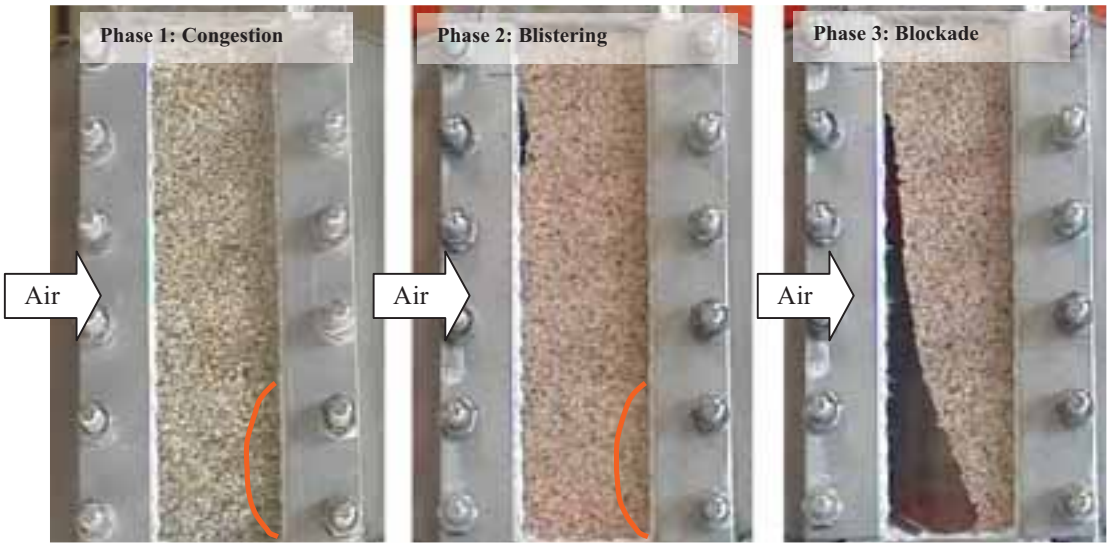


**Fig. 12: Blocking behaviour of bulk flow in three phases**

## 4. Conclusions

As particle degradation is an important design aspect, a variety of candidate materials has been investigated with respect to thermal, thermo-mechanical, and tribological properties. It turns out that the effective thermal bulk conductivity of all investigated materials behaves independently of the corresponding solid's conductivity. It is mainly influenced by grain size and temperature, and also by porosity and thermal conductivity of the solid and the gaseous phase. Natural stones, in particular quartz sand, have a low resistance to thermal shock, which limits the applicable range of temperature and temperature changes. Technical ceramics, like alumina or bauxite, do not exhibit any sensitivity to thermal cycling.

Attrition occurs for all materials under investigation except for alumina grinding balls thanks to their hardness, strength and round shape. Quartz flint shows the least proneness to attrition and reaches a stagnating attrition fraction after a large shear strain. Corundum and bauxite generate much wear debris after a short time of loading. Si-SiC honeycombs are highly resistant to abrasion thanks to its dense structure and tensile strength, other than porous Re-SiC. Metallic meshes should only be applied if fiber ends can be protected from the moving bulk.

The analysis of the pressure drop that occurs when air is passing through the particle bed reveals that the average grain size should be at least 1 mm. Air velocities that lead to blocking of the sand flow range from 1.4 m/s to 2.1 m/s with increasing average grain size and particle roundness. There is no obvious dependence of the critical air velocity on the sand mass flow rate.

The blocking behavior of bulk flows was investigated. As a result the dependence of three blocking states on the bulk material as well as the dependence on air mass flow could be detected and quantified.

Presently the most promising bulk materials are basalt, quartz, and bauxite (Norpro). Further investigations at high temperatures (about 600 °C) will be carried out before final decisions will be made.

## 5. Acknowledgements

The work was funded by the German Federal Ministry for the Environment, Nature Conservation and Nuclear Safety (BMU) under contracts no. 0325119A and B. This financial support is gratefully acknowledged.

## 6. References


Hoffschmidt, B., 2003. Patents DE000010149806C2, 30.4.2003 and DE000010208487A1, 18.9.2003

Bridgwater, J., 2007. Particle Breakage due to Bulk Shear, in: Ghadiri, M., Hounslow, M., Salman, A.D. (Eds.), Handbook of Powder Technology, Volume 12, Chapter 3. Elsevier Science and Technology.

Ghadiri, M., Ning, Z., Kenter, S.J., Puik, E., 2000. Attrition of granular solids in a shear cell. Chemical Engineering Science 55, 5445-5456.

Hoffschmidt, B., 1997. Comparison and Evaluation of Different Concepts of Volumetric Radiation Receivers, Doctoral Thesis RWTH Aachen, DLR Forschungsbericht 97-35, 1997

Warerkar, S., Schmitz, S., Goettsche, J., Hoffschmidt, B., Reißel, M., Tamme, R., 2011. Air-Sand Heat exchanger for high-temperature storage. Journal of Solar Energy Engineering (ASME), Vol. 133, May 2011